0026-895X/86/010058-11$02.00/0

MOLECULAR PHARMACOLOGY, 30:58-68

Gallamine Binding to Muscarinic M1 and M2 Receptors, Studied by Inhibition of [^{3}H]Pirenzepine and [^{3}H]Quinuclidinylbenzilate Binding to Rat Brain Membranes

ROBERT E. BURKE

Department of Neurology, Columbia University, New York, New York 10032

Received September 13, 1985; Accepted February 24, 1986

SUMMARY

Whereas classic muscarinic antagonist ligands appear to recognize only a single class of muscarinic receptor sites, the recently discovered antagonist pirenzepine appears to distinguish at least two classes of sites. Its unique binding properties, demonstrated in both indirect and direct binding studies, have led to an emerging concept of high affinity (M1) and low affinity (M2) sites. This concept has been supported by pharmacologic studies of functional muscarinic responses, as well as by data suggesting different effector relationships for the two sites. Gallamine possesses muscarinic antagonist properties, and it also recognizes heterogeneity among muscarinic receptors. The purpose of this study was to define gallamine-recognized heterogeneity in terms of the pirenzepine-defined M1, M2 concept. This has been done by studying the ability of gallamine to inhibit [^{3}H]pirenzepine binding to the M1 site, and to inhibit [^{3}H]quinuclidinylbenzilate ([^{3}H]QNB) binding in cerebellar membrane preparations, which contain almost exclusively the M2 site. The results show that gallamine binds with high affinity to the M2 site, with K_i = 2.4 nM, and lower affinity to the M1 site with K_i = 24 nM. Within these classes gallamine does not recognize heterogeneity. The ability of gallamine to inhibit [^{3}H]QNB binding to cortex is best described by a two-site model comprised of 77% low affinity gallamine sites (M1) and 23% high affinity gallamine sites (M2). Thus, the heterogeneity among muscarinic receptors which is recognized by gallamine within the receptor binding paradigms of this study can be attributed to the M1, M2 subtypes as defined by pirenzepine binding. In addition, gallamine at low concentrations appears to bind as a pure competitive antagonist at these two sites, indicated by linear Schild plots with slopes of 1.0, the lack of an effect on dissociation of radioligands, and the ability to protect [^{3}H]pirenzepine and [^{3}H]QNB-binding sites from alkylation by propylbenzylcholine mustard. These studies do not exclude the possibility of a non-competitive interaction of gallamine with the muscarinic receptor observed by other investigators at high gallamine concentrations, and postulated to occur at a site adjacent to the primary muscarinic site. It is proposed that gallamine is capable of interacting with both the primary muscarinic site and an allosteric site. These results support the emerging concept of M1 and M2 muscarinic subclasses and suggest that gallamine and related compounds may be useful in defining muscarinic receptor subclasses, given their higher affinity for the M2 site.

Until recently, most receptor binding studies of muscarinic antagonists have revealed interaction with a single class of sites, for a variety of antagonists in several tissues (1, 2). Studies of agonists have revealed more complex interactions, believed to be due, at least in part, to conformational constraints imposed by membrane proteins on the ligand-binding site (3, 4). Although some early data suggested that antagonists may also recognize heterogeneity, as evidenced by their small, but definite, regional differences in brain-binding properties (5), nevertheless, most early binding evidence favored the concept of a single class of sites.

This work was supported by National Institute of Neurological and Communicative Disorders and Stroke Teacher-Investigator Award 1 K07 NS00746-02, the Dystonia Medical Research Foundation, and the Parkinson's Disease Foundation.

More recently, however, the *in vitro* receptor binding and the pharmacologic properties of pirenzepine have provided substantial evidence for muscarinic receptor heterogeneity for an antagonist. Indirect binding studies show a variation in affinity for pirenzepine among peripheral tissues and among brain regions (6). Forebrain structures show a high affinity for pirenzepine and Hill coefficients <1, whereas medulla-pons shows low affinity and a Hill coefficient of 1.0. This indirect evidence for regional heterogeneity of brain muscarinic antagonist-binding sites has been supported by direct studies of [^{3}H]Pir binding, which have shown in both homogenate (7–9) and intact tissue preparations (10), that there is a greater proportion of high affinity pirenzepine-binding sites in forebrain than in hindbrain. Consistent with the results of binding studies, pharmacologic studies have revealed selective effects of pirenzepine

ABBREVIATIONS: [^{3}H]Pir, [^{3}H]pirenzepine; [^{3}H]QNB, [^{3}H]quinuclidinylbenzilate; [^{3}H]NMS, [^{3}H]*N*-methylscopolamine; PBCM, propylbenzylcholine mustard.

on functional responses. Pirenzepine has a greater potency to inhibit gastric acid secretion (11) and ganglionic stimulation (12) than to induce tachycardia. In brain, pirenzepine appears to be a more potent antagonist of acetylcholine at presynaptic receptors regulating dopamine release than at those regulating acetylcholine release (13). Based on this evidence of a selective action of pirenzepine, a nomenclature of M1, for high affinity pirenzepine sites, and M2, for low affinity sites, has been proposed (12), in accord with an earlier nomenclature which was based on the selectivity of muscarinic agonists in a lower esophageal sphincter preparation (14). Gilbert *et al.* (15) have recently shown that the M1, M2 nomenclature based on agonist selectivity is compatible with that based on pirenzepine selectivity. The concept of M1 and M2 muscarinic receptor subtypes has been further strengthened by evidence suggesting different effector mechanism associations for the two subtypes on two cultured cell lines (16). Although it is not clear that the M1 and M2 muscarinic receptor subtypes, defined by pirenzepine binding, represent different receptor proteins (17, 18), nevertheless, the concept of these subtypes appears to be a useful one at present to describe available pharmacological evidence.

It has been known for many years that gallamine, in addition to its nicotonic cholinergic blocking properties, has antimuscarinic properties which appear to be selective for the heart (19–22). These pharmacologic studies have been supported by indirect studies of gallamine binding which have shown a greater effect in heart than in other tissues (23). In brain, gallamine demonstrates a regional heterogeneity in its ability to inhibit radioligand binding which is the opposite of that of pirenzepine; it has a higher affinity for hindbrain than for forebrain membrane preparations (23, 24). This inverse relationship between gallamine and pirenzepine binding in brain tissue and heart suggests that the heterogeniety among muscarinic receptors recognized by gallamine may be related to that recognized by pirenzepine. One purpose of this study, therefore, was to attempt to define gallamine-recognized heterogeneity in terms of the M1, M2 classification defined by pirenzepine binding in brain membrane preparations. This has been done by inhibition experiments in two muscarinic ligand binding paradigms: gallamine inhibition of [^{3}H]Pir binding in forebrain, and inhibition of [^{3}H]QNB binding in cerebellum. The former paradigm provides a measure of gallamine interaction with the M1 site, because in filtration assays [^{3}H]Pir binds to a single site, indicated by linear Scatchard plots, with a single high affinity equal to that for the M1 site (8, 9). The binding of [^{3}H]QNB to cerebellar membranes is primarily to M2 sites, as [^{3}H]Pir binding is 10% of less of total muscarinic binding (8, 9).

Another issue related to gallamine's antimuscarinic pharmacology is whether it acts as a competitive or noncompetitive antagonist. Whereas some pharmacologic studies have shown pure competitive antagonist (21), others have shown, at high gallamine doses, nonlinear relationships on Schild plots (22). Similarly, controversy exists in studies of receptor binding. Ellis and Hoss (24) concluded that gallamine acts as a competitive antagonist. Stockton *et al.* (23) found that gallamine inhibition of [^{3}H]NMS was characterized by nonlinear Schild plots, and that gallamine slowed [^{3}H]NMS dissociation, findings consistent with noncompetitive antagonism possibly due to allosteric modulation of binding. Similar findings were noted by Dunlap and Brown (25) in a study of gallamine inhibition of [^{3}H]QNB binding to heart membrane preparations. A second purpose of this study, therefore, was to reexamine the nature of gallamine antagonism of muscarinic binding with attention to the possibility of different modes of interaction with muscarinic receptor subtypes.

Experimental Procedures

Materials. [^{3}H]Pir (82.3 Ci/mmol; lot 2039-137) and PBCM were obtained from New England Nuclear. [^{3}H]-L-QNB (38 Ci/mmol; batches 20, 21) was obtained from Amersham. Pirenzepine dihydrochloride was a kind gift of Thomae GmbH, West Germany. Gallamine triethiodide, atropine sulfate, buffer reagents, and polyethyleneimine were obtained from Sigma Chemical Co.

Membrane preparations and binding assays. Membranes were prepared for both [^{3}H]Pir and [^{3}H]QNB assays as described by Watson *et al.* (8), with minor modifications. Male Sprague-Dawley rats (225–260 g; Charles River Breeding Laboratories) were killed by decapitation on the day of assay. Brains were rapidly removed and placed on an ice-chilled glass plate. Brain regions were rapidly dissected, weighed, and homogenized on ice with a Polytron (Brinkmann) homogenizer setting 6, for 15 sec in 20.0 ml of iced 10.0 mM sodium-potassium phosphate buffer (pH 7.5). The homogenization step was repeated after a 30-sec wait. This crude membrane homogenate was further diluted in 10 mM $NaKPO_4$ (pH 7.5) according to the particular assay and brain region (100 volumes/g of wet weight for [^{3}H]Pir, forebrain regions; 700–900 volumes for [^{3}H]QNB, cortex; 80 volumes for [^{3}H]QNB, cerebellum).

For assay of [^{3}H]Pir binding, 100 μl of this membrane homogenate were incubated in a final volume of 2.0 ml with [^{3}H]Pir (0.6–8.0 nM) in 10 mM $NaKPO_4$ (pH 7.5) for 60 min at 25°. Nonspecific binding was defined by the addition of 1 μM atropine sulfate to the incubation. The incubation was stopped by addition of 5.0 ml of iced 10 mM $NaKPO_4$ and then immediate filtration through Whatman GF/B (2.5 cm) glass fiber filters, under a vacuum of 15 in. Hg. Filters had been soaked previously in 0.1% polyethylenimine for 30 min. The filters were washed with two 5.0-ml volumes of iced buffer. Filters were then air-dried and placed in plastic scintillation vials with 10.0 ml of Aquasol fluor (New England Nuclear). After the vials had stood for at least 6 hr, radioactivity was counted in a refrigerated Packard liquid scintillation counter at an efficiency of 40%. Under these assay conditions, specific [^{3}H]Pir binding was saturable, with a linear Scatchard plot analysis, a Hill coefficient approximately equal to 1, and an affinity constant of 3–4 nM, as reported (8, 9). Total specific binding was linear for tissue concentrations ranging from 10 to 250 μg of protein/ml of incubate. Because gallamine has been reported to significantly slow the rate of association of muscarinic antagonist ligands (23), its effect on time to reach equilibrium for [^{3}H]Pir binding was examined in cortex, striatum, hippocampus, and medulla-pons membrane preparations at concentrations of gallamine up to 100 nM. Although slowing of association was noted, equilibrium was reached at 60 min (Fig. 1A).

For assay of [^{3}H]QNB binding, membranes were prepared on the day of assay, as described above, and 200 μl of membrane homogenate were incubated in a final volume of 8.0 ml with [^{3}H]QNB (8–70 pM) in 10 mM $NaKPO_4$ buffer for 3 hr at 25°. Nonspecific binding was defined by addition of 1 μM atropine sulfate. The incubation was terminated by addition of 5.0 ml of iced buffer, followed by immediate filtration and two 5.0-ml washes, as for the [^{3}H]Pir assay, except that filters had not been soaked in polyethylenimine. Filters were dried and counted in 10.0 ml of Aquasol at an efficiency of 37%. Under these conditions, specific [^{3}H]QNB binding was saturable, with a linear Scatchard plot, a Hill coefficient approximately equal to 1, and an affinity constant of 8 pM. Total specific binding was linear, with tissue concentrations ranging from 5.0 to 40 μg of protein/assay. Pilot studies showed that gallamine significantly slows the rate of association of [^{3}H]QNB, such that an incubation time of 3 hr was required (Fig. 1, B and C). There was no significant loss of binding at these incubation times, and others have shown that gallamine is not metabolized (23).

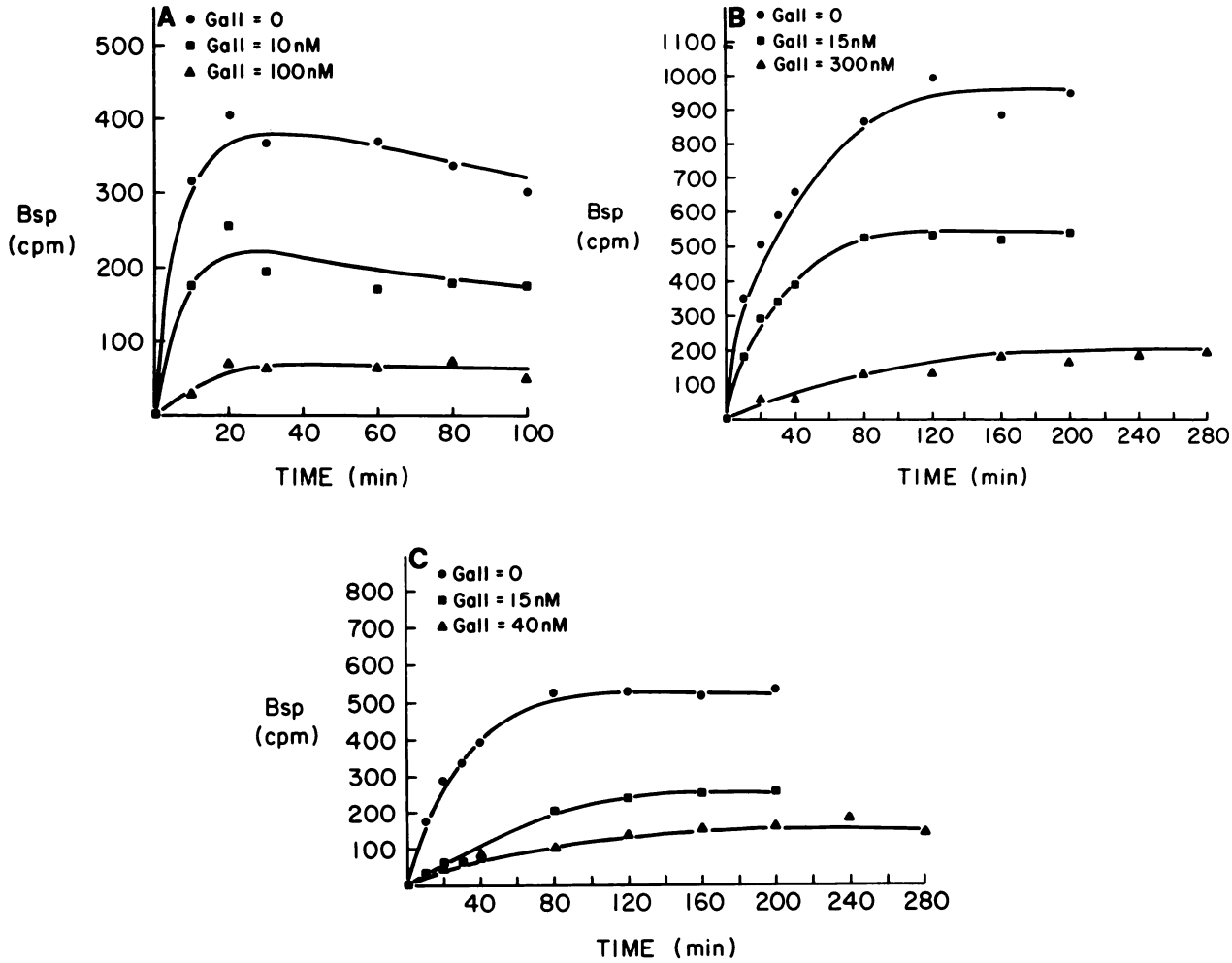

Fig. 1. The effect of gallamine on the rate of association of [^{3}H]Pir and [^{3}H]QNB. A. The effect of varying concentrations of gallamine on the rate of association of [^{3}H]Pir to membranes prepared from rat cortex. Cortex membranes were prepared as described in Experimental Procedures and incubated at a final mean protein concentration of 50 μg/ml with 0.6 nM [^{3}H]Pir. Two-ml aliquots were assayed in triplicate for total binding by rapid filtration as described, at the times indicated. Nonspecific binding was constant with time and has been subtracted from total binding to give specific binding (*Bsp*) as shown. Equilibrium was achieved by 60 min incubation. Beyond that period, progressive decline in specific binding was noted. Similar results were obtained for striatum and hippocampus (data not shown). Curves were fitted by hand. B. The effect of gallamine at 15 nM and 300 nM on the rate of association of [^{3}H]QNB to membranes prepared from rat cortex. In the gallamine = 0 and 15 nM conditions, cortical membranes were incubated at a final mean protein concentration of 8 μg/ml with 6 pM [^{3}H]QNB, at a final incubation volume of 8.0 ml. At the times indicated, total binding was determined in triplicate by rapid filtration as described in Experimental Procedures. The experiment was performed twice, and mean specific binding (*Bsp*) from the two studies is shown. In the gallamine = 300 nM condition, the same membrane protein and [^{3}H]QNB concentrations were used, but to maintain adequate counts in the presence of this high concentration of gallamine, an incubation volume of 24 ml was used. Prior to the start of incubation, each tube containing 24 ml was brought into thermal equilibrium at 25°. Equilibrium of binding was achieved at 180 min incubation in all conditions. Curves were hand fitted. C. The effect of gallamine at 15 nM and 40 nM on the rate of association of [^{3}H]QNB to membranes prepared from rat cerebellum. In the gallamine = 0 and 15 nM conditions, cerebellar membranes were incubated at a final mean protein concentration of 150 μg/ml with 6 pM [^{3}H]QNB, at a final incubation volume of 8.0 ml. At the times indicated, total binding was determined by rapid filtration. As described above for cortex, in the gallamine = 300 nM condition, the same concentrations of protein and gallamine were used, but to increase the number of counts retained on the filter, the incubation volume was increased to 24 ml. Equilibrium of binding was achieved at 180 min incubation in all conditions. Curves were hand fitted.

Dissociation time experiments were performed by incubating membranes with [^{3}H]Pir or [^{3}H]QNB for 60 min in the presence or absence of gallamine, then adding atropine sulfate to a final concentration of 1 μM, and then terminating the reaction by rapid filtration at varying times afterwards. Nonspecific binding, defined by incubation with 1 μM atropine, was constant as a function of time.

Alkylation of muscarinic receptors with PBCM. For all experiments with PBCM, it was allowed to cyclize to the aziridinium ion by incubation in 10 mM $NaKPO_4$ buffer (pH 7.5) at room temperature for 40 min, at a concentration of 0.6 mM (26, 27). The reaction was stopped by a 10-fold dilution with iced buffer. Pilot studies determined the optimal conditions for alkylation of muscarinic receptors, compatible with subsequent determination of [^{3}H]Pir and [^{3}H]QNB binding. Binding was less variable when performed on freshly prepared brain membranes, as described above. Incubation with varying concentrations of PBCM at 25° for 60 min showed that maximal inhibition (70–80%) of [^{3}H]QNB binding occurred at 40 nM PBCM, and no additional inhibition was noted at 400 nM; thus, 20–30% of [^{3}H]QNB binding seemed resistant to alkylation as noted by others (28). A 15-min preincubation of membranes at 25° with varying concentrations of pirenzepine demonstrated the ability of pirenzepine to protect both [^{3}H]QNB- and [^{3}H]Pir-binding sites from alkylation. To selectively alkylate low affinity pirenzepine sites, a "protecting" concentration of 200 nM pirenzepine was chosen. The effectiveness of this protocol to produce a membrane preparation relatively enriched in high affinity [^{3}H]Pir sites was indicated by an increase in pirenzepine affinity in

indirect studies (see Fig. 7). PBCM was able to alkylate [^{3}H]QNB sites in both cortex (predominantly M1) and cerebellar (predominantly M2) membrane preparations, but it appeared to be more effective in cerebellar preparations, consistent with prior results (28). Pretreatment of membranes with pirenzepine followed by treatment with PBCM did not result in a change in the K_D of either [^{3}H]Pir or [^{3}H]QNB for the remaining binding sites. Treatment of cortical membranes with PBCM alone, without pirenzepine pretreatment, did not result in a change in the K_D of [^{3}H]QNB for the remaining sites, or the ability of pirenzepine or gallamine to inhibit [^{3}H]QNB binding to these sites. Exposure of cortical membranes to the incubation conditions of the alkylation experiment (1 hr, 15 min at 25°) without the addition of pirenzepine or PBCM did not affect the K_D of [^{3}H]Pir or [^{3}H]QNB, or the ability of gallamine to inhibit [^{3}H]QNB.

Protein determinations. Proteins were measured using the Lowry technique (29), with bovine serum albumin as standard.

Data analysis. Inhibition data were analyzed by linear regression analysis of log-logit plots for determination of IC_{50} values and Hill coefficients. K_i values were calculated from IC_{50} values with use of the Cheng-Prusoff equation (30). In the PBCM alkylation experiments, differences in linear regression line slopes and intercepts were tested for significance by use of the Student's t test for differences in regression coefficients. Inhibition data were also analyzed by a nonlinear least squares curve-fitting procedure, for which the LIGAND program (31) was converted to Applesoft by Dr. M. H. Teicher and generously provided by the Biomedical Computing Technology Information Center at Vanderbilt Medical Center. All experiments for a particular condition were fit simultaneously to derive binding parameters for that condition, and the program correction factor (C) for inter-experiment variation in total binding was allowed to vary. For these analyses the affinity constants of the labeled ligands, which had been determined empirically in separate experiments, were held constant at the empirical values. No other parameters, including binding capacity, competing ligand affinity, or nonspecific binding, were constrained for the curve fitting. The derived value for maximal binding always agreed with values expected on empirical grounds. The fit for gallamine inhibition of specific [^{3}H]QNB was enhanced by allowing the program to "fit" nonspecific binding, rather than defining nonspecific binding purely on empirical grounds by 1 μM atropine. This difference has been interpreted to mean that, in an inhibition experiment where a lipophobic unlabeled ligand (such as gallamine) is inhibiting a lipophilic labeled ligand (such as [^{3}H]QNB), a large excess of another lipophilic, unlabeled compound (in this case, atropine) may not provide an appropriate definition of nonspecific binding.

LIGAND defined nonspecific binding only for the models depicted in Figs. 5 and 6; in all other studies, nonspecific binding was defined empirically by 1 μM atropine. For the gallamine inhibition of [^{3}H]Pir, there was no difference in analysis between empiric and "fitted" definitions of nonspecific binding.

Data showing the effect of gallamine on radiolabeled ligand affinity (determined by linear regression analysis of Scatchard plots) were plotted according to the Schild equation:

$$\log(x - 1) = \log[I] - \log K_i$$

where $[I]$ is the concentration of competitive antagonist, K_i is the dissociation constant at equilibrium of the antagonist, and x is the affinity shift induced by the antagonist, i.e., $x = K_D$ (in the presence of antagonist)/K_D (in its absence).

Dissociation time data were expressed according to the equation

$$\ln B/B_0 = -k_{-1}t$$

where B_0 = amount bound at time zero, B = amount bound at time t, and k_{-1} equals the dissociation rate constant. Dissociation time data expressed in this form were analyzed by linear regression analysis, and k_{-1} was determined from the slope. Best fit lines for gallamine and no gallamine conditions were compared by the Student's t statistic for differences in regression coefficients.

Results

Gallamine inhibition of [^{3}H]Pir binding. Gallamine concentrations of 1 μM or greater completely inhibited the binding of [^{3}H]Pir to cortex membrane preparations (Fig. 2, *inset*). The ability of gallamine to inhibit [^{3}H]Pir binding was similar in cortex, striatum, and hippocampus membrane preparations, as shown in Fig. 2, A and B. K_i values for gallamine, calculated from the IC_{50} values, ranged from 28 to 30 nM for

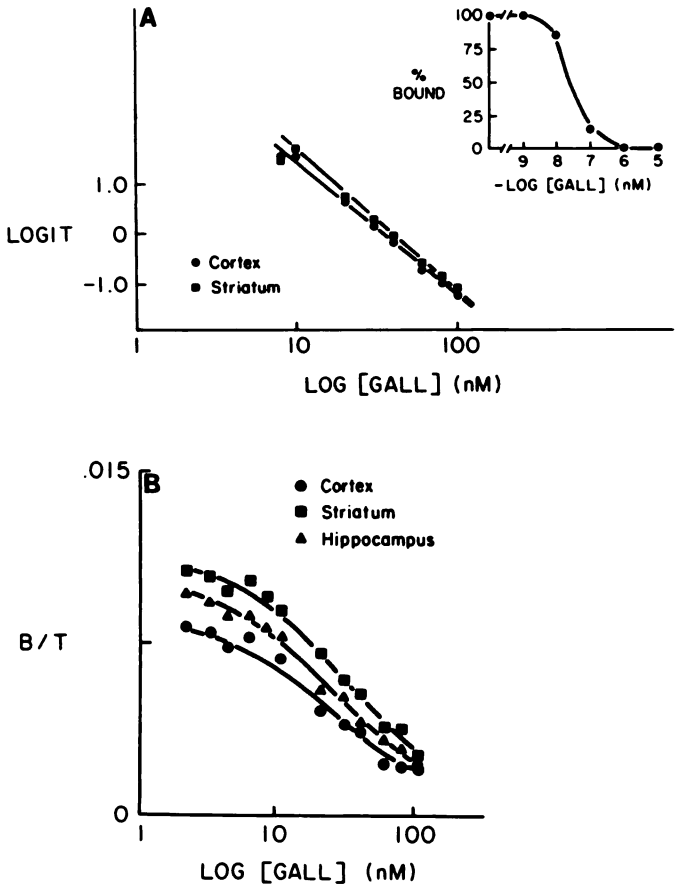

Fig. 2. Inhibition of [^{3}H]Pir binding by gallamine in cortex, striatum, and hippocampus membrane preparations. A. Linear regression analysis of log-logit plots of gallamine inhibition data for cortex and striatum. Data for hippocampus were similar and have been deleted for clarity. Each *point* for cortex (●) is the mean of four experiments performed in quadruplicate. For striatum (■) (and hippocampus, not shown) each *point* is the mean of three experiments performed in triplicate. In these experiments protein concentration was approximately 50 μg/ml, and [^{3}H]Pir was 0.2 nM. Analysis revealed:

	r	IC_{50} (nM)	K_i (nM)	n_H
Cortex	−0.99	33	28	1.2
Striatum	−0.99	35	30	1.1
Hippocampus	−0.99	33	28	1.2

The *inset* shows the results of a single experiment demonstrating the ability of high concentrations of gallamine to completely inhibit [^{3}H]Pir binding. B. LIGAND model curves for cortex (●), striatum (■), and hippocampus (▲). Each *curve* is based on all experimental data for each region; the *points* represent data from single, representative experiments. Binding of [^{3}H]Pir is expressed on the *ordinate* as *B/T* (bound [^{3}H]Pir/total [^{3}H]Pir). In this and all of the following figures, "Bound" refers to specific binding. Each curve is based on a single-site model, and the K_D for [^{3}H]Pir was held constant at an empirically determined value of 3.3 nM. Model values for K_i for gallamine were: cortex = 24 ± 2 nM; striatum = 29 ± 2 nM; hippocampus = 23 ± 2 nM.

the three regions, in agreement with K_i values derived by the LIGAND program, assuming a single-site mass action model, which ranged from 23 to 29 nM. Hill coefficients for the inhibition data for the three regions did not significantly differ from 1, suggesting a noncooperative interaction with a single class of binding sites. Two-site models did not offer an enhanced fit of the data.

Analysis of gallamine inhibition of [^{3}H]Pir binding to hindbrain (medulla-pons) membrane preparations was made difficult by the small amount of specific binding in this region. Six displacement experiments performed in triplicate showed complete inhibition of [^{3}H]Pir binding at gallamine concentrations greater than 1 μM. At 10 nM gallamine there was 85 ± 12% [^{3}H]Pir binding; at 100 nM, 41 ± 12%; at 1000 nM, 15 ± 8%. Thus, gallamine binds to M1 sites in hindbrain regions with an affinity approximately equal to that for forebrain regions.

Gallamine inhibition of [^{3}H]QNB binding. Because prior studies have shown tissue concentration to affect apparent QNB affinity in both direct (2) and indirect (9) binding experiments, the effect of tissue concentration on gallamine inhibition of [^{3}H]QNB binding (Fig. 3) was examined. There was an inverse relationship between tissue concentration and the IC_{50} for gallamine inhibition. The following inhibition experiments were performed at the lowest tissue levels compatible with reproducible inhibition data (3 μg of protein/ml for cortex, 140 μg/ml for cerebellum).

Gallamine was a more potent inhibitor of [^{3}H]QNB binding in cerebellum than in cortex (Fig. 4). In cerebellum, gallamine had a calculated K_i of 2.5 nM, whereas in cortex the K_i was 17 nM. This difference was not due to the lower concentration of muscarinic binding sites in cerebellum because, for these experiments, cerebellum was studied at a higher protein (and receptor) concentration than was cortex. In addition, even when the IC_{50} for cortex is obtained by extrapolation to zero tissue concentration (see Fig. 3), it remains greater than that for cerebellum. Neither the Hill coefficient for cerebellum (0.98) nor that for cortex (0.90) differed appreciably from 1.0. A single-site model for gallamine inhibition of [^{3}H]QNB binding in cerebellum was supported by nonlinear least-squares curve fitting, as shown in Fig. 5. This single-site model was achieved with a K_i of 2.4 ± 0.2 nM.

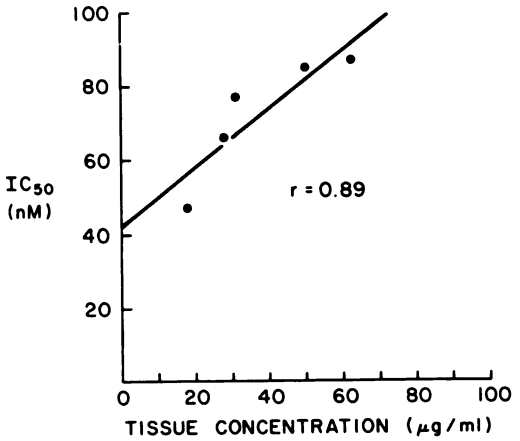

Fig. 3. The effect of increasing tissue concentration on the IC_{50} for gallamine inhibition of [^{3}H]QNB binding to cortex. Each *point* represents the IC_{50} value determined from a linear regression analysis of log-logit inhibition data. [^{3}H]QNB concentration was 20 pM in all experiments. Each tissue concentration was studied by two experiments performed in triplicate. There is an inverse relationship between tissue concentration and IC_{50} ($r = -0.89$). Extrapolating to zero indicates a "true" IC_{50} value of 42 nM. Ligand depletion ranged from 8% at the lowest tissue concentration to 25% at the highest.

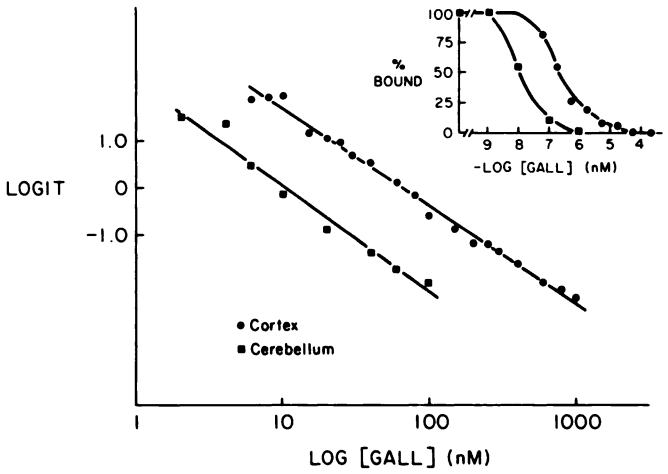

Fig. 4. Inhibition of [^{3}H]QNB binding by gallamine in cortex and cerebellum. Linear regression analysis of log-logit plots of gallamine inhibition data for cortex (●) and cerebellum (■). Each *point* represents the mean of two experiments performed in triplicate. For experiments with cortex, protein concentration was approximately 3 μg/ml ([receptor] = 3 pM), and with cerebellum, 140 μg/ml ([receptor] = 4 pM). [^{3}H]QNB = 24 pM. For cortex, $r = -0.99$, IC_{50} = 66 nM (calculated K_i = 17 nM), and n_H = 0.90. For cerebellum, $r = -0.99$, IC_{50} = 10 nM (calculated K_i = 25 nM), and n_H = 0.98. The *inset* shows that, at high concentrations, gallamine completely inhibited the binding of [^{3}H]QNB in both cortex and cerebellum (protein = 9 μg/ml in the cortex study).

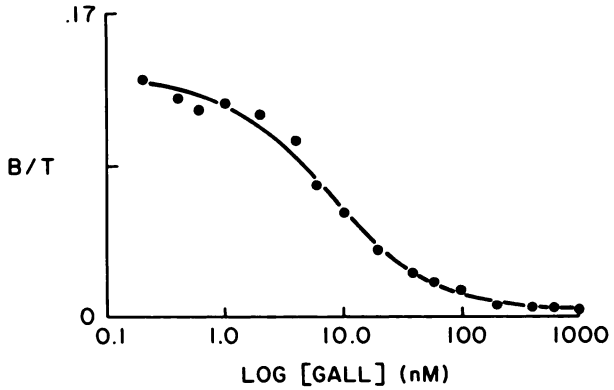

Fig. 5. Inhibition of [^{3}H]QNB binding by gallamine in cerebellum. The theoretical inhibition curve was fitted to the same data shown in Fig. 4 (two experiments performed in triplicate), but the *points* are from a single representative experiment. For the analysis, the K_D for [^{3}H]QNB was held constant at an empirically determined value of 8 pM. The model value for the K_i of gallamine was 2.4 ± 0.2 nM.

Fig. 6 shows that gallamine inhibition of [^{3}H]QNB binding to cortex can be described by a single-site model with a K_i of 17 ± 1 nM. Since this affinity is intermediate between that of gallamine for the M1 site (24 nM, Fig. 2) and the M2 site (2.4 nM, Fig. 5), the degree of fit for a two-site model with these binding parameters was also examined, as shown in Fig. 6. A fit approximately equal to the one-site model was achieved with relative proportions of 77% for the low affinity site and 23% for the high affinity site. Although it is customary to reject a two-site model as less parsimonious when it does not improve the description of the data provided by a one-site model, it is apparent that the anticipated difference in gallamine affinity

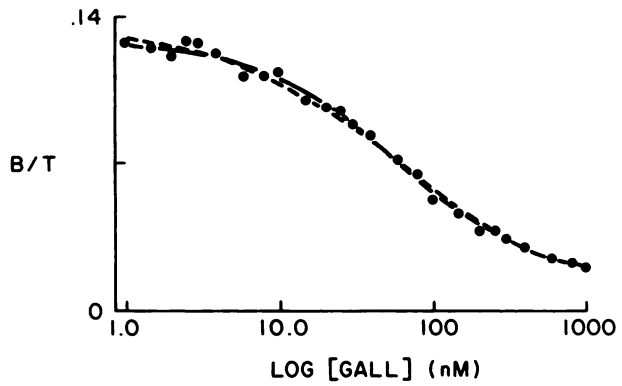

Fig. 6. Inhibition of [^{3}H]QNB binding by gallamine in cortex. The theoretical inhibition curves for a one-site model (——) and a two-site model, assuming K_{i_H} = 2.4 nM and K_{i_L} = 24 nM (– – –) were fitted to the same data shown in Fig 3 (two experiments performed in triplicate). The *points* represent the means for the experiments. The K_D for [^{3}H]QNB was held constant at 8 pM. For the single-site model, a K_i for gallamine of 17 ± 1 nM was obtained. For the two-site model, receptor concentrations of R_H = 0.7 ± 0.1 pM and R_L = 2.4 ± 0.1 pM were obtained. The two models fit the data almost equally well, with a final mean square residual variance of 31.1 and 35.6 for the one- and two-site models, respectively.

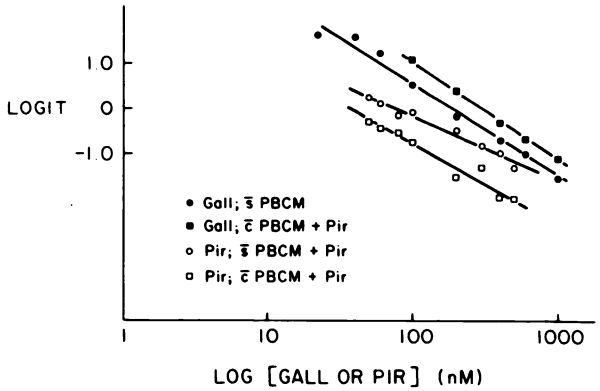

Fig. 7. The effect of selective, irreversible blockage of low affinity pirenzepine (M2) sites by PBCM on pirenzepine and gallamine inhibition of [^{3}H]QNB binding. Low affinity sites for pirenzepine were selectively alkylated by preincubating cortex membranes (5 mg/ml) with 200 nM pirenzepine, and then adding 40 nM PBCM. The reaction was stopped by cooling to 4° and immediate centrifugation, followed by a single wash with iced buffer, and resuspension of membranes in buffer. Then, 200 μl of this alkylated membrane preparation were added to a final incubate volume of 8.0 ml (final protein concentration of 7 μg/ml). The effect of this protocol on the displacement of [^{3}H]QNB (64 pM) by pirenzepine is shown by parallel experiments in which membranes were subjected to the protocol either without (○) or with (□) PBCM treatment. In both conditions, membranes were pretreated with pirenzepine to control for any possible retention of pirenzepine by the membranes following the wash steps. It can be seen that there is a significant ($p < 0.001$) shift to the left following M2 blockade. Following treatment with this protocol, there is a significant ($p < 0.05$) shift to the right of the gallamine inhibition curve. Points for gallamine inhibition following no PBCM treatment (●) represent the means of three experiments; points for inhibition following PBCM treatment (■) represent means of two experiments, all performed in triplicate. The same experiments performed in parallel showed identical results (data not shown). As indicated in Experimental Procedures, exposure of cortical membranes to the incubation conditions of the alkylation experiment without the addition of pirenzepine or PBCM did not affect the K_D of [^{3}H]Pir or [^{3}H]QNB or the ability of gallamine to inhibit [^{3}H]QNB binding.

for the two sites recognized in cortex is too small to be resolved by computer modeling of inhibition binding data. Therefore, to further study the one- and two-site models for gallamine binding to cortical membranes, the effect of selective irreversible blockade of M2 sites on gallamine inhibition of [^{3}H]QNB binding in cortex was examined.

Fig. 7 shows the effect of selective irreversible blockade of low affinity pirenzepine sites (M2) with PBCM on the ability of pirenzepine and gallamine to inhibit [^{3}H]QNB binding to cortical membranes. As expected, this treatment results in a shift of the pirenzepine inhibition curve to the left ($p < 0.001$), presumably due to the relative increase of M1 sites. There is a tendency for the Hill coefficient to approach 1.0 following PBCM (n_H = 0.6 without PBCM, n_H = 0.8 with PBCM), but this does not achieve significance ($p < 0.2$). Following selective blockade of low affinity pirenzepine sites in cortex, there is a significant shift ($p < 0.05$) of the gallamine inhibition curve to the right. This suggests that gallamine recognizes heterogeneity among cortical muscarinic receptors and that a two-site model is the appropriate one for description of gallamine inhibition of [^{3}H]QNB binding in cortex.

Gallamine inhibition of [^{3}H]Pir and [^{3}H]QNB binding: Schild plot analysis. To study whether gallamine inhibits muscarinic binding by a competitive or noncompetitive mechanism, the effect of increasing gallamine concentration on affinity constants of [^{3}H]Pir and [^{3}H]QNB was studied. In Fig. 8, A and B, the effect of increasing gallamine concentration on [^{3}H]Pir binding is shown. The progressive increase in the K_D of [^{3}H]Pir associated with increasing gallamine concentration is linear and close to a theoretical Schild plot for a competitive interaction (Fig. 8B). As noted in Fig. 8A, the B_{max} at 300 nM gallamine is an assumed value of 36 pM, because of the technical difficulty of determining B_{max} empirically at binding levels only 18% of those in the absence of gallamine. The Schild plot-derived K_i for gallamine binding at cortical high affinity pirenzepine sites, 29 nM, is in agreement with that obtained by inhibition experiments (Fig. 2, A and B).

Gallamine inhibition of [^{3}H]QNB binding in cortex also is due to a competitive interaction; a Schild plot is linear with a slope of 1.1 (Fig. 9, A and B). At a gallamine concentration of 300 nM, [^{3}H]QNB binding was reduced to 40% of that in the absence of gallamine. Similarly, gallamine inhibition of [^{3}H]QNB binding in cerebellum conformed to a simple, competitive model (Fig. 10, A and B).

The effect of gallamine on the dissociation rates of [^{3}H]Pir and [^{3}H]QNB. Gallamine has previously been reported to slow the rate of dissociation of muscarinic antagonist ligands (23, 25). Since such an effect cannot be attributed to a purely competitive interaction, the effect of gallamine on [^{3}H]Pir and [^{3}H]QNB dissociation was studied. Membranes were incubated with radiolabeled ligand alone, or with ligand plus gallamine, and rate of dissociation was measured following addition of 1 μM atropine. Thus, the rate of dissociation of radiolabeled ligand bound alone is compared to its dissociation rate in the presence of bound gallamine, the latter evidenced by partial inhibition of radiolabeled ligand binding at time = 0. In this paradigm, gallamine showed no effect on the rate of dissociation of [^{3}H]Pir from cortex (Fig. 11) or of [^{3}H]QNB from cortex or cerebellum (Fig. 12). Thus, these studies showed no evidence of a noncompetitive interaction between gallamine and these antagonist ligands.

The ability of gallamine to protect [^{3}H]Pir- and [^{3}H]QNB-binding sites from alkylation by PBCM. If gallamine is a competitive antagonist of [^{3}H]Pir and [^{3}H]QNB binding, then it should protect their binding sites from irre-

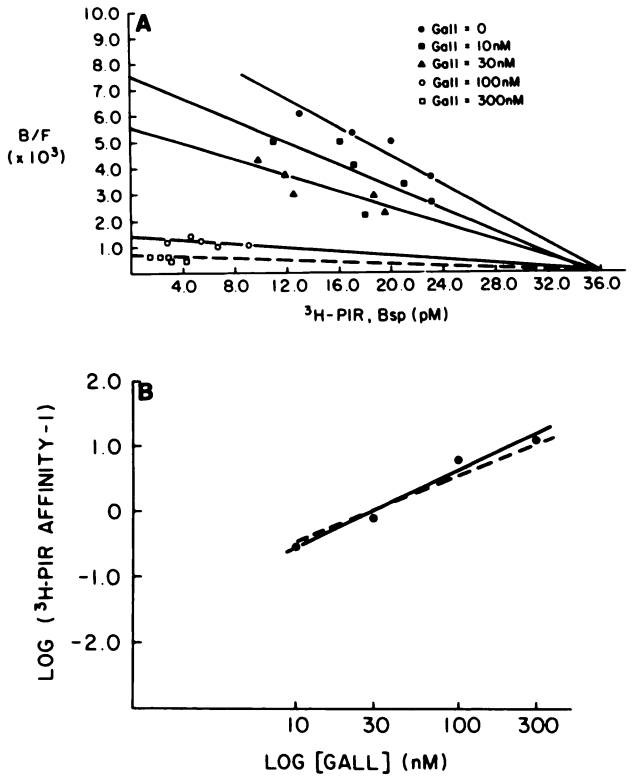

Fig. 8. The effect of increasing gallamine concentration on the binding affinity of [^{3}H]Pir in cortex. A. Scatchard plots of [^{3}H]Pir binding at different gallamine concentrations are shown. The *points* show values determined in triplicate. Experiments were performed in pairs, in parallel, with the exception of the 300 nM condition. [^{3}H]Pir concentrations ranged from 2.0 to 8.0 nM. At 300 nM, gallamine reduced specific binding to 18% of that obtained in the absence of gallamine. At this low level of [^{3}H]Pir binding, it was difficult to determine B_{max}, because nonspecific binding greatly exceeded specific binding at [^{3}H]Pir greater than 8.0 nM. Therefore, because no concentration of gallamine up to 100 nM had influenced B_{max}, it was treated at 300 nM gallamine as 36 pM, and the K_D was derived to be 51 nM. – – –, "derived" Scatchard plot at 300 nM; —, linear regression fits of Scatchard plots. B. Schild plot analysis of the data shown in A, and summarized as follows (*, derived):

Gall (nM)	K_D (nM)	B_{max} (pM)	K_D shift
0	3.6	36	
10	4.6	35	1.3
30	6.4	36	1.8
100	27	38	7.4
300	51*		14.2

It can be seen that the data lie along a line (——), with a K_i of 29 nM and a slope of 1.2. The best fit line for the data is not significantly different from a theoretical line based on a K_i of 29 nM and assuming a competitive interaction (– – –).

versible alkylation with PBCM. To study this prediction, cortical and cerebellar membranes were treated with varying concentrations of gallamine, and then PBCM, as shown in Table 1. Increasing concentrations of gallamine offered increasing protection from alkylation by PBCM. At 1000 nM gallamine, protection of cortical high affinity [^{3}H]Pir sites was almost complete. Although these experiments did not demonstrate complete protection of [^{3}H]QNB binding, they do not exclude the ability of gallamine to do so because membranes were examined only at a single time point (60 min) of incubation with PBCM. A complete evaluation of protection ability would require assessment of binding after shorter incubation times.

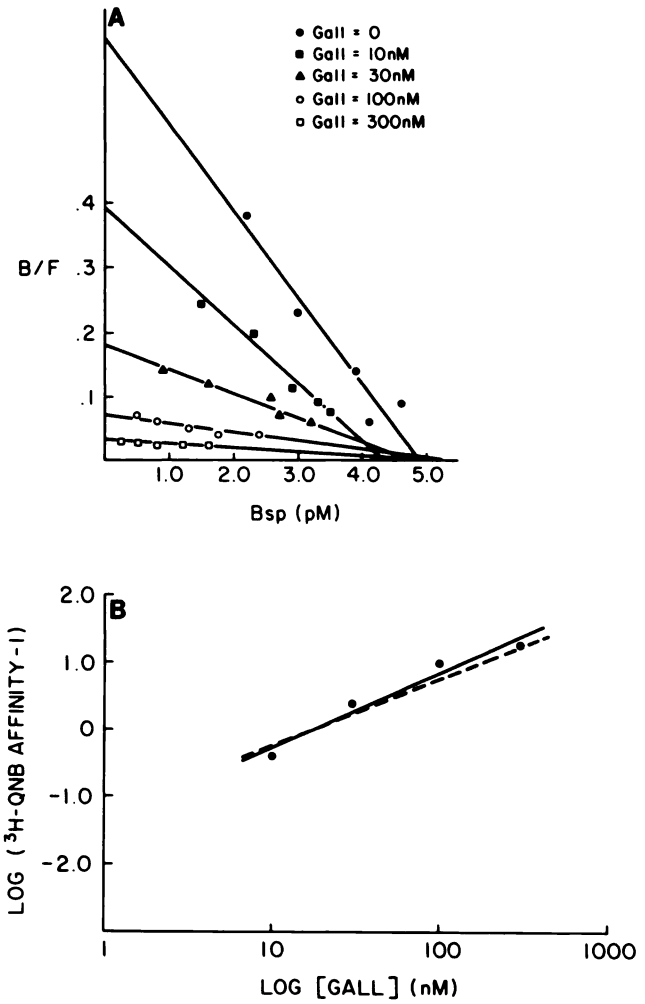

Fig. 9. The effect of increasing gallamine concentration on the binding affinity of [^{3}H]QNB in cortex. A. Scatchard plots of [^{3}H]QNB binding at different gallamine concentrations are shown. The *points* show representative experiments performed in triplicate; each was repeated with similar results. Experiments were performed in pairs, in parallel. [^{3}H]QNB concentration ranged from 8 to 70 pM. B. Schild plot of the data shown in A, and summarized as follows:

Gall (nM)	K_D (pM)	B_{max} (pM)	K_D shift
0	8.0	4.9	
10	11	4.3	1.4
30	27	4.8	3.4
100	81	5.4	10.1
300	158	5.3	19.8

The points lie along a straight line with a K_i of 18 nM. The best fit line for the data (—) is not significantly different from a theoretical line based on a K_i of 18 nM and a competitive interaction (– – –).

Discussion

In a filtration assay, specific [^{3}H]Pir binding is predominantly to the high affinity pirenzepine (M1) site, indicated by linear Scatchard plots, with Hill coefficients approximately equal to 1.0, with the affinity anticipated for the M1 site (8, 9). In addition, at the highest concentrations of [^{3}H]Pir used in these studies (8–9 nM), only minimal binding to the low affinity site would be expected, where pirenzepine has an affinity of about 200 nM (9). Finally, the anticipated rate of dissociation for the low affinity M2 site would be so rapid as to make binding in a filtration assay negligible (32). Therefore, the

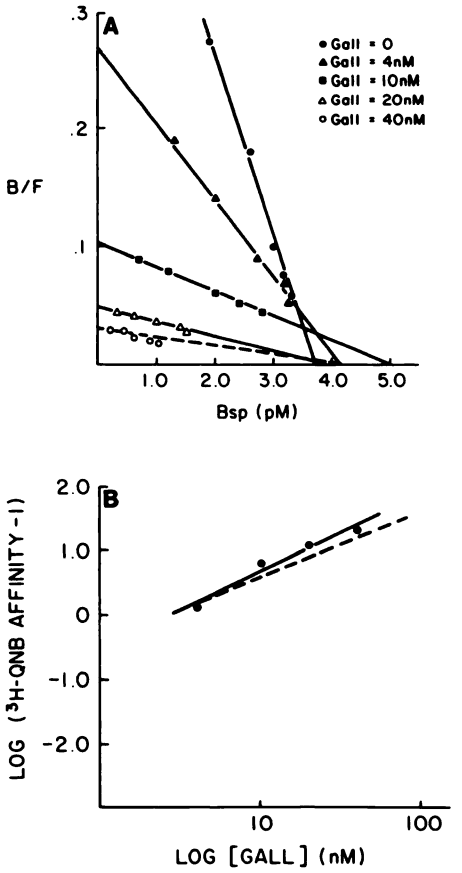

Fig. 10. The effect of gallamine on binding of [^{3}H]QNB in cerebellum. A. Representative Scatchard plots in the presence of varying concentrations of gallamine. As explained in Fig. 8A, the B_{max} in the presence of 40 nM gallamine was assumed to be 4.0 pM, and the K_D was derived. B. Schild plot based on the data shown in A (•, derived):

Gall (nM)	K_D (pM)	B_{max} (pM)	K_D shift
0	6.5	3.7	
4	15	4.1	2.3
10	50	5.0	7.7
20	81	3.8	12.5
40	137*		21.0

The linear regression analysis line (—) lies close to a theoretical line for a competitive interaction and a K_i of 2.7 nM (– – –).

inhibition of [^{3}H]Pir binding by gallamine can be considered a measure of interaction with the M1 site. The results presented here show that gallamine inhibits [^{3}H]Pir binding in cortex according to a model which assumes a competitive interaction with a single site, with K_i = 24 ± 2 nM. Gallamine inhibits [^{3}H]Pir binding in a similar fashion in striatum, hippocampus, and medulla-pons. The competitive nature of gallamine's interaction with the M1 site is supported by a Schild plot analysis of gallamine's effect on [^{3}H]Pir affinity, which shows a progressive, linear affinity shift with increasing gallamine. This competitive model is further supported by experiments showing the lack of an effect on [^{3}H]Pir dissociation, and the ability of gallamine to protect [^{3}H]Pir sites from alkylation by PBCM.

Others have shown that there is a very small amount of [^{3}H]Pir binding to cerebellum (8, 9) and that [^{3}H]QNB binding in this region is primarily to the low affinity (M2) pirenzepine site. In cerebellum, gallamine inhibition of [^{3}H]QNB binding is modeled by a competitive interaction with a single site, with

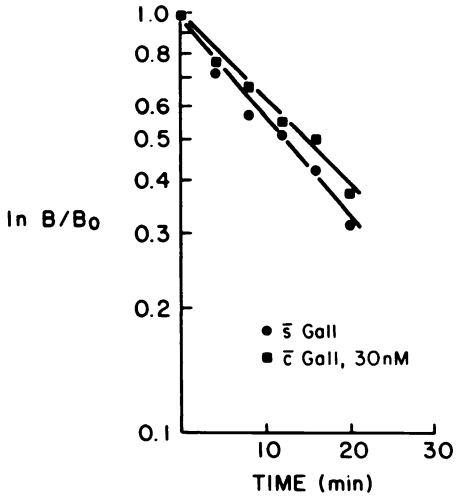

Fig. 11. The effect of gallamine on [^{3}H]Pir dissociation in cortex. The dissociation rate of [^{3}H]Pir was studied in the absence (●) and the presence (■) of gallamine. Each *point* represents the mean of two experiments, performed in parallel, each in triplicate. Cortical membranes (50 μg of protein/ml of incubate) were incubated with 1 nM [^{3}H]Pir either alone or in the presence of 300 nM gallamine. At time = 0, atropine was added to a final concentration of 1 μM, and at the times shown, incubates were vacuum filtered and washed. Gallamine 30 nM reduced specific binding at time = 0 by about 50%. Linear regression analysis of data from each condition showed k_{-1} = 0.054 min^{-1} in the absence of gallamine, and k_{-1} = 0.046 min^{-1} in the presence of gallamine, not a significant difference.

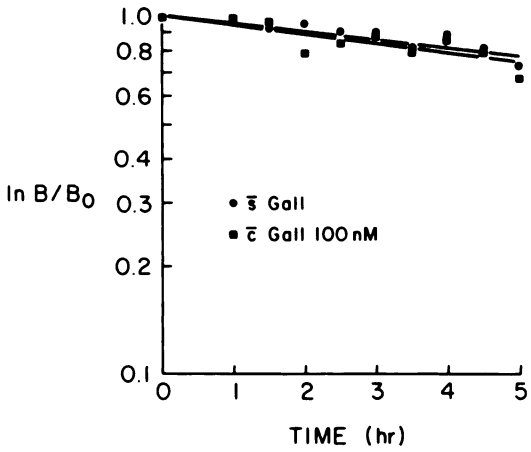

Fig. 12. The effect of gallamine on [^{3}H]QNB dissociation in cortex. The dissociation rate of [^{3}H]QNB was studied in the absence (●) and presence (■) of 100 nM gallamine. Each *point* represents the mean of two experiments, performed in parallel, each in triplicate. Cortical membranes (9 μg of protein/ml of incubate) were incubated with 80 pM [^{3}H]QNB, with or without gallamine, at 25° for 1 hr, at which time (defined as t = 0) atropine was added to a final concentration of 1 μM. Then, 8.0-ml aliquots were removed at the times shown and assayed for total binding. Nonspecific binding was constant as a function of time. Also assayed in parallel were incubates which did not have atropine added at t = 0; these showed that there was no loss of specific binding, in either the absence or presence of gallamine, during the course of the experiment. At t = 0, specific binding in the gallamine 100 nM condition showed $t_{1/2}$ = 12.0 hr in the absence of gallamine and 10.7 hr in its presence—not a significant difference. Similar studies of cortical membranes at 12 pM [^{3}H]QNB and 30 and 15 nM gallamine showed identical results, as did studies of cerebellar membranes at 12 pM [^{3}H]QNB and 5 nM gallamine.

TABLE 1

Protection of [^{3}H]Pir and [^{3}H]QNB binding by gallamine against alkylation with PBCM

Membranes were incubated at room temperature for 15 min with 0, 50, 100, or 1,000 nM gallamine and then with or without 40 nM PBCM for 60 min. The membrane suspensions were then immediately centrifuged at 40,000 × *g* for 10 min at 4°. The pellet was resuspended in 200 volumes/original wet weight of iced buffer for cortex or 80 volumes for cerebellum, and then centrifuged again and resuspended in the same volumes. [^{3}H]Pir and [^{3}H]QNB were then measured as described in Experimental Procedures at 8.4 nM and 64 pM, respectively, for all five conditions shown below, in parallel. Each value below represents the mean of two separate experiments, with specific and nonspecific binding determined in triplicate for each condition. As noted by others (28), some [^{3}H]QNB sites were resistant to blockade by PBCM.

Pretreatment		Percentage of Total binding		
		Cortex		Cerebellum
PBCM	Gallamine	[^{3}H]QNB	[^{3}H]Pir	[^{3}H]QNB
nM				
0	0	100	100	100
40	0	39	29	18
40	50	49	56	59
40	100	69	54	63
40	1000	79	96	78

K_i = 2.4 ± 0.2 nM. As with [^{3}H]Pir binding in cortex, the competitive nature of gallamine's interaction with cerebellar M2 sites is supported by Schild plot analysis, the lack of an effect on dissociation, and the ability of gallamine to protect cerebellar [^{3}H]QNB sites from PBCM.

The interaction of gallamine with [^{3}H]QNB in cortex membrane preparations requires interpretation. Pirenzepine recognizes two classes of muscarinic receptor in cortex membrane preparations (6, 8, 9); approximately 65% are the high affinity (M1) type (9) [although estimates by others, using different criteria for M1 binding, range up to 85% (33)]. Since experiments described above have demonstrated the ability of gallamine to bind with different affinities to the M1 and M2 sites, it would be expected that gallamine would similarly recognize this heterogeneity in cortex. However, the difference in gallamine affinity for these two sites is small, being a single order of magnitude. Thus, one would anticipate greater difficulty in demonstrating a two-site model for gallamine than for pirenzepine, which has approximately a 2-order of magnitude affinity difference for these sites. A 20–25% proportion of one site, which differs in affinity by 10-fold from the second site in a two-site model, is at the limit of resolution of a computer modeling approach, even for an experimentally ideal system (34). Fig. 6 shows that a single site and the appropriate two-site model for gallamine displacement of [^{3}H]QNB in cortex are barely distinguishable. It is notable that the optimal two-site model for gallamine, obtained with an affinity of 2.4 nM for M2 sites and 24 nM for M1 sites, is achieved by proportions of 77% M1 and 23% M2, the approximate expected proportions if gallamine indeed recognized the same heterogeneity as pirenzepine. To attempt to distinguish between the one- and two-site models, the approach of selective blockade of pirenzepine-recognized subclasses was used. The results show that when cortical membranes are incubated with PBCM in the presence of 200 nM pirenzepine, there is selective alkylation of low affinity pirenzepine sites, as indicated by an increase in pirenzepine affinity. In membranes treated this way, the affinity of gallamine binding, measured by inhibition of [^{3}H]QNB, decreases. If the single-site model for gallamine binding in cortex is correct, this should not occur; selective elimination of low affinity pirenzepine sites should have no effect on gallamine binding. On the basis of this experiment, it is apparent that gallamine recognizes muscarinic receptor heterogeneity in cortex which is related to pirenzepine-recognized heterogeneity, and that gallamine has a lower affinity for the high affinity pirenzepine site. The most parsimonious model of gallamine binding, therefore, is that gallamine binds with different affinity to M1 and M2 sites, at affinities of 24 and 2.4 nM, respectively, and that it recognizes no heterogeneity within these classes. Gallamine binding to cortex is described by a two-site model with the above affinities, with proportions of 77% and 23% for M1 and M2. The greater affinity of gallamine for hindbrain than forebrain membranes, as found here and by others (23, 24), is due to the preponderance of M1 sites in forebrain.

These results are compatible with the main findings of Ellis and Hoss (24), who found that gallamine competitively inhibits [^{3}H]QNB binding and that there is a regional heterogeneity for gallamine binding, with a higher affinity in hindbrain. One major difference, however, is that the present results did not demonstrate a low affinity (50–100 μM) site for gallamine in forebrain or hindbrain. The results here show essentially complete inhibition of [^{3}H]QNB binding at 100 nM in cerebellum and 1000 nM in cortex, whereas Ellis and Hoss (24) noted only 60% inhibition of binding at these concentrations for the two regions. The reason for this difference is not apparent; possibly relevant are methodologic differences related to membrane preparation (in the present study only fresh membranes were used), or incubation time (3 hr in the present study). There is a correspondence between what Ellis and Hoss (24) reported as the magnitude of affinity difference for high affinity sites in hindbrain and forebrain, 25 and 150 nM, respectively, and the results reported here, i.e., 2.4 and 24 nM, respectively, for cerebellum and cortex. The difference between the two studies in the values for these high affinity sites is similar in magnitude to the difference between the two studies in the K_D for [^{3}H]QNB, i.e., 50 pM (24) and 8 pM (Fig. 8A). This suggests an underlying methodological difference as responsible for the quantitative affinity differences. It has been shown, for example, that [^{3}H]QNB has a higher affinity in 10 mM $NaKPO_4$ than in 50 nM $NaKPO_4$ (8). An additional point of agreement between the results here and those reported by Ellis and Lenox (35) is the lack of an effect of gallamine on the [^{3}H]QNB dissociation rate.

Stockton *et al.* (23) provided strong evidence that gallamine interacts noncompetitively with [^{3}H]NMS in heart and cerebral cortex. They showed that gallamine was not able to completely displace [^{3}H]NMS at high concentrations, that Schild plots of gallamine inhibition of [^{3}H]NMS binding were nonlinear, and that gallamine slowed the rate of dissociation. In none of these respects, however, did the present results suggest a noncompetitive interaction between gallamine and [^{3}H]QNB in brain. One possible explanation for this disparity of findings is that [^{3}H]NMS and [^{3}H]QNB interact with muscarinic receptors in fundamentally different ways, as recently suggested by Ellis and Lenox (28). They proposed that gallamine and quaternary ammonium muscarinic antagonists both recognize a low affinity site where an allosteric interaction between these compounds can occur, at high concentrations. This interpretation would explain why, in the present study, where low concentrations of both gallamine and [^{3}H]QNB have been used, and only

high affinity gallamine sites have been studied, a purely competitive interaction was observed. It is noteworthy that in the study of Stockton *et al.* (23), the most significant deviations from mass action took place at [^{3}H]NMS concentrations 3–8-fold greater than its K_D. In addition, tissue (and receptor) concentrations were high, at 1 mg of protein/ml. Under these circumstances, high concentrations of gallamine would be required to demonstrate inhibition (32), and it is possible that, at these concentrations, an allosteric interaction predominates.

This concept, that [^{3}H]QNB and [^{3}H]NMS fundamentally differ in their muscarinic binding properties, cannot, however, be invoked to reconcile the present findings with those of Dunlap and Brown (25), who concluded that gallamine interacts noncompetitively in heart membranes with [^{3}H]QNB. Like Stockton *et al.* (23), they observed an inability of gallamine to completely inhibit [^{3}H]QNB binding and an ability to slow [^{3}H]QNB dissociation. They also noted that gallamine did not protect [^{3}H]QNB sites from alkylation. It is possible that in cardiac tissue the relationship between gallamine and [^{3}H]QNB binding differs from that in brain. It is also possible that methodological considerations as discussed above are at least partially responsible for the differences between their findings and those presented here. The concentration of [^{3}H]QNB used by Dunlap and Brown (25) in competition studies ranged from 0.15 to 1.9 nM, and the concentration of receptor was approximately 30 pM (880 fmol/mg of protein; 40 μg of protein/ml), whereas in the present study, concentrations of [^{3}H]QNB and receptor were 24 and 5 pM, respectively. On theoretical grounds (32), and demonstrated empirically for receptor concentration (Fig. 3), the higher concentration conditions would increase the concentration of gallamine required to demonstrate inhibition. It is possible that, at these high concentrations of gallamine, the interaction with the muscarinic receptor becomes a noncompetitive one. Indeed, Dunlap and Brown (25) demonstrated that gallamine induces noncompetitive behavior only at concentrations greater than or equal to 30 μM.

A scheme for gallamine's interaction with the muscarinic receptor, which attempts to account for the present results and those of other investigators, would postulate that gallamine is capable of both competitive and noncompetitive interaction; the former is observed exclusively at low gallamine concentrations, and the latter becomes apparent at high concentrations. At low gallamine concentrations, muscarinic receptor heterogeneity is recognized, and the subpopulations correspond to those recognized by pirenzepine, but with an opposite affinity relationship. This difference in the affinity of gallamine for the M1 and M2 subtypes, defined by pirenzepine binding, accounts for the regional heterogeneity of brain gallamine binding. At higher concentrations, gallamine is able to demonstrate allosteric effects on the primary muscarinic ligand-binding site, perhaps by binding at an adjacent site. A similar scheme, postulating interaction with both the primary ligand-binding site and an adjacent site, with allosteric effects, has been proposed for clomiphene (36). A model based on simultaneous binding of two ligands at the muscarinic receptor has also been proposed for scopolamine and pirenzepine, based on studies performed at high concentrations of [^{3}H]QNB and competing ligands (37). The physiologic significance of an allosteric interaction of gallamine with the primary site is, at present, unknown.

The results obtained here with PBCM suggest that the high and low affinity sites recognized by pirenzepine in cortex are independent, noninteracting sites. In the presence of pirenzepine, PBCM selectively alkylated low affinity pirenzepine sites, demonstrated by an increased affinity of pirenzepine for the remaining nonalkylated sites. This selective alkylation resulted in a decreased affinity for gallamine, which suggests that the sites differentiated by gallamine are also independent. The demonstration here of affinity shifts supports the concept that the two receptor subclasses can be independently studied. These results and conclusions are not incompatible with the additional concept that, at high concentration, gallamine may act at another site to allosterically modify binding and induce heterogeneity (25).

In conclusion, gallamine studied at low concentration appears to bind competitively at the muscarinic receptor site. It recognizes subclasses of muscarinic receptors, and this heterogeneity can be explained in terms of the heterogeneity also recognized by pirenzepine. Thus, the binding properties of gallamine lend additional support to the emerging concept of M1 and M2 muscarinic subclasses. Since gallamine is unique among muscarinic antagonists for having a higher affinity at the M2 site, it (or related compounds, such as pancuronium) may prove useful in further characterization of muscarinic receptors. Up to now, definition of M2 binding has depended on indirect studies with pirenzepine, or with carbachol (33). The binding of agonists, however, is complicated by relationships with effector mechanisms. The availability of M2-selective antagonists would possibly provide a simpler, more direct approach to the characterization of M2 binding and to the general classification of muscarinic receptors.

Acknowledgments

I am grateful to Ms. Anne K. Finnerty for excellent technical assistance, and to Alexa Macedonia for diligent preparation of the manuscript.

References

1. Hulme, E. C., N. J. M. Birdsall, A. S. V. Burgen, and P. Mehta. The binding of antagonists to brain muscarinic receptors. *Mol. Pharmacol.* **14**:737–750 (1978).
2. Fields, J. Z., W. R. Roeske, E. Morkin, and H. I. Yamamura. Cardiac muscarinic cholinergic receptors. *J. Biol. Chem.* **253**:3251–3258 (1978).
3. Birdsall, N. J. M., A. S. V. Burgen, and E. C. Hulme. The binding of agonists to brain muscarinic receptors. *Mol. Pharmacol.* **14**:723–736 (1978).
4. Birdsall, N. J. M., E. C. Hulme, and A. S. V. Bergen. The character of the muscarinic receptors in different regions of the rat brain. *Proc. R. Soc. Lond. B Biol. Sci.* **207**:1–12 (1980).
5. Kloog, Y., Y. Egozi, and M. Sokolovsky. Characterization of muscarinic acetylcholine receptors from mouse brain: evidence for regional heterogeneity and isomerization. *Mol. Pharmacol.* **15**:545–558 (1979).
6. Hammer, R., C. P. Berrie, N. J. M. Birdsall, A. S. V. Burgen, and E. C. Hulme. Pirenzepine distinguishes between different subclasses of muscarinic receptors. *Nature (Lond.)* **283**:90–92 (1980).
7. Watson, M., W. R. Roeske, and H. I. Yamamura. [^{3}H]Pirenzepine selectively identifies a high affinity population of muscarinic cholinergic receptors in the rat cerebral cortex. *Life Sci.* 31:2019–2023 (1982).
8. Watson, M., H. I. Yamamura, and W. R. Roeske. A unique regulatory profile and regional distribution of [^{3}H]pirenzepine binding in the rat provide evidence for distinct M1 and M2 muscarinic receptor subtypes. *Life Sci.* **32**:3001–3011 (1983).
9. Luthin, G. R., and B. B. Wolfe. Comparison of [^{3}H]pirenzepine and [^{3}H]quinuclidinylbenzilate binding to muscarinic cholinergic receptors in rat brain. *J. Pharmacol. Exp. Ther.* **228**:648–655 (1984).
10. Wamsley, J. K., D. R. Gehlert, W. R. Roeske, and H. I. Yamamura. Muscarinic antagonist binding site heterogeneity as evidenced by autoradiography after direct labeling with [^{3}H]-QNB and [^{3}H]-pirenzepine. *Life Sci.* **34**:1395–1402 (1984).
11. Hirschowitz, B. I., J. Fong, and E. Molina. Effects of pirenzepine and atropine on vagal and cholinergic gastric secretion and gastrin release and on heart rate in the dog. *J. Pharmacol. Exp. Ther.* **225**:263–268 (1983).
12. Hammer, R., and A. Giachetti. Muscarinic receptor subtypes: M1 and M2 biochemical and functional characterization. *Life Sci.* **31**:2991–2998 (1982).
13. Raiteri, M., R. Leardi, and M. Marchi. Heterogeneity of presynaptic musca-

rinic receptors regulating neurotransmitter release in the rat brain. *J. Pharmacol. Exp. Ther.* **228**:209–214 (1984).
14. Goyal, R. K., and S. Rattan. Neurohumoral, hormonal, and drug receptors for the lower esophageal sphincter. *Gastroenterology* **74**:598–619 (1978).
15. Gilbert, R., S. Rattan, and R. K. Goyal. Pharmacologic identification, activation and antagonism of two muscarine receptor subtypes in the lower esophageal sphincter. *J. Pharmacol. Exp. Ther.* **230**:284–291 (1984).
16. Evans, T., M. M. Smith, L. I. Tanner, and T. K. Hardin. Muscarinic cholinergic receptors of two cell lines that regulate cyclic AMP metabolism by different molecular mechanisms. *Mol. Pharmacol.* **26**:395–404 (1984).
17. Venter, J. C. Muscarinic cholinergic receptor structure. *J. Biol. Chem.* **258**:4842–4848 (1983).
18. Roeske, W. R., and J. C. Venter. The differential loss of [^{3}H]pirenzepine vs. [^{3}H](−)-quinuclidinylbenzilate binding to soluble rat brain muscarinic receptors indicates that pirenzepine binds to an allosteric state of the muscarinic receptor. *Biochem. Biophys. Res. Commun.* **118**:950–957 (1984).
19. Riker, W. F., and W. C. Wescoe. The pharmacology of Flaxedil, with observations on certain analogs. *Ann. N. Y. Acad. Sci.* **54**:373–392 (1951).
20. Laity, J. L. H., and B. K. Garg. A note on the action of gallamine on isolated rabbit auricles. *J. Pharm. Pharmacol.* **14**:371–373 (1962).
21. Rathburn, F. J., and J. T. Hamilton. Effect of gallamine on cholinergic receptors. *Can. Anaesth. Soc. J.* **17**:574–590 (1970).
22. Clark, A. L., and F. Mitchelson. The inhibitory effect of gallamine on muscarinic receptors. *Br. J. Pharmacol.* **58**:323–331 (1976).
23. Stockton, J. M., N. J. M. Birdsall, A. S. V. Burgen, and E. C. Hulme. Modification of the binding properties of muscarinic receptors by gallamine. *Mol. Pharmacol.* **23**:551–557 (1983).
24. Ellis, J., and W. Hoss. Competitive interaction of gallamine with multiple muscarinic receptors. *Biochem. Pharmacol.* **31**:873–876 (1982).
25. Dunlap, J., and J. H. Brown. Heterogeneity of binding sites on cardiac muscarinic receptors induced by the neuromuscular blocking agents gallamine and pancuronium. *Mol. Pharmacol.* **24**:15–22 (1983).
26. Young, J. M., R. Hiley, and A. S. V. Burgen. Homologues of benzilylcholine mustard. *J. Pharm. Pharmacol.* **24**:950–954 (1972).
27. Burgen, A. S. V., C. R. Hiley, and J. M. Young. The binding of [^{3}H]-propylbenzilylcholine mustard by longitudinal muscle strips from guinea pig small intestine. *Br. J. Pharmacol.* **50**:145–151 (1974).
28. Ellis, J., and R. H. Lenox. Quaternary forms of classical muscarinic antagonists distinguish subpopulations of muscarinic receptors. *Biochem. Biophys. Res. Commun.* **126**:1242–1258 (1985).
29. Lowry, O. H., N. J. Rosebrough, A. L. Farr, and R. J. Randall. Protein measurement with the Folin phenol reagent. *J. Biol. Chem.* **193**:165–175 (1951).
30. Cheng, Y., and W. H. Prusoff. Relationship between the inhibition constant (*Ki*) and the concentration of inhibitor which causes 50 percent inhibition (IC_{50}) of an enzymatic reaction. *Biochem. Pharmacol.* **22**:3099–3108 (1973).
31. Munson, P. J., and D. Rodbard. LIGAND: a versatile computerized approach for characterization of ligand-binding systems. *Anal. Biochem.* **107**:220–239 (1980).
32. Bennet, J. P. Methods in binding studies, in *Neurotransmitter Receptor Binding* (H. I. Yamamura, S. J. Enna, and M. J. Kuher, eds). Raven Press, New York, 57–90 (1978).
33. Potter, L. T., D. D. Flynn, H. E. Hanchett, D. L. Kalinoski, J. Luber-Narod, and D. C. Mash. Indepedent M1 and M2 receptors: ligands, autoradiography and functions. *Trends Pharmacol. Sci.* (suppl.) 22–31 (1984).
34. De Lean, A., A. A. Hancock, and R. J. Leftkowitz. Validation and statistical analysis of a computer modeling method for quantitative analysis of radioligand binding data for mixtures of pharmacological receptor subtypes. *Mol. Pharmacol.* **21**:5–16 (1982).
35. Ellis, J., and R. H. Lenox. Characterization of the interacting of gallamine with muscarinic receptors from brain. *Biochem. Pharmacol.* **34**:2214–2217 (1985).
36. Ben-Baruch, G., G. Schreiber, and M. Sokolovsky. Cooperativity pattern in the interaction of the antiestrogenic drug clomiphene with the muscarinic receptors. *Mol. Pharmacol.* **21**:287–295 (1982).
37. Hedlund, B., M. Grynfarb, and T. Bartfaz. Two ligands may bind simultaneously to the muscarinic receptor. *Naunyn Schmiedeberg's Arch. Pharmacol.* **320**:3–13 (1982).

Send reprint requests to: Dr. Robert E. Burke, Department of Neurology, Columbia University, Box 67, Neurological Institute, 710 West 168th Street, New York, NY 10032.